

Recent Results from $2\pi^0$ Photoproduction off the Proton

Martin Kotulla, for the TAPS and A2 Collaborations

Department of Physics and Astronomy, University of Basel, CH-4056 Basel (Switzerland)

Abstract. The reaction $\gamma p \rightarrow \pi^0 \pi^0 p$ has been measured using the TAPS BaF₂ calorimeter at the tagged photon facility of the Mainz Microtron accelerator in the beam energy range from threshold up to 820 MeV. Close to threshold, chiral perturbation theory (ChPT) predicts that this channel is significantly enhanced compared to double pion final states with charged pions. The strength is attributed dominantly to pion loops in the $2\pi^0$ channel - a finding that opens new prospects for the test of ChPT. Our measurement is the first which is sensitive enough for a conclusive comparison with the ChPT calculation and is in agreement with its prediction. The data are also in agreement with a calculation in the unitary chiral approach.

In the second resonance region, a recent model interpretation of new GRAAL data claimed a dominance of the $P_{11}(1440) \rightarrow \sigma N$ reaction process. We present very accurate invariant mass distributions of $\pi^0 \pi^0$ and $\pi^0 p$ systems, which are in contrast to the σN intermediate state and which show a dominance of the $\Delta \pi$ intermediate state.

INTRODUCTION

The description of the low energy properties of the nucleon as well as the study of nucleon resonances remain a long-standing task of hadronic physics. The unique features of the $2\pi^0$ channel - the strong suppression of the direct production (Δ Kroll-Rudermann, Born terms, . . .) - open new prospects to improve the knowledge in both fields.

Chiral Perturbation Theory

In the low energy regime where properties of the lowest lying baryons and mesons are studied, an approach exploiting the approximate Goldstone boson nature of the pion has been developed: chiral perturbation theory (ChPT) [1, 2]. This effective field theory has been extended to the nucleon sector (HBChPT¹) [3, 4]. In general, it turns out, that ChPT is in good agreement with experiment in describing $\pi - N$ scattering [5]. From the study of $\pi\pi$ production processes, complementary information to the study of the single pion photoproduction channels can be gained. ChPT predicts that the $\pi^0 \pi^0$ photoproduction channel is strongly enhanced due to chiral (pion) loops [6] which appear in leading (non vanishing) order q^3 . This is a counter-intuitive result, since in the case of single pion production the cross sections for charged pions are considerably larger than the ones

¹ ChPT is used in this paper as a synonym for HBChPT

with neutral pions in the final state. In a calculation up to order M_π^2 , the pion loops at order q^3 are responsible for two thirds of the total cross section [7]. This fact makes this channel unique, because unlike in other channels where the loops are adding some contribution to the dominant tree graphs, here they are absolutely dominating. In [7], the following prediction for the near threshold cross section was given:

$$\sigma_{tot}(E_\gamma) = 0.6 \text{ nb}((E_\gamma - E_\gamma^{thr})/10 \text{ MeV})^2 \quad (1)$$

where E_γ denotes the photon beam energy and E_γ^{thr} the production threshold of 308.8 MeV. The largest resonance contribution at order M_π^2 comes from the $P_{11}(1440)$ resonance via the $N^*N\pi\pi$ s-wave vertex. Actually, the uncertainty of the coupling of the $P_{11}(1440)$ to the s-wave $\pi\pi$ channel was a limiting factor for the accuracy of the ChPT calculation [7]. Therefore, for the most extreme case of this coupling, an upper limit for this cross was given in addition by increasing the constant in Eq. 1 from 0.6 nb to 0.9 nb.

Completing the overview of theoretical calculations of the reaction $\gamma p \rightarrow \pi^0\pi^0 p$ close to threshold, this channel is also described in a recent version of the Gomez Tejedor-Oset model [8]. This model is based on a set of tree level diagrams including pions, nucleons and nucleonic resonances. In a recent work, particular emphasis was put on the re-scattering of pions in the iso-spin $I=0$ channel [9]. Double pion photoproduction via the Δ Kroll-Rudermann term is not possible for the $2\pi^0$ final state. In case of a $\pi^-\pi^+$ Kroll-Rudermann term, the charged pions can re-scatter into two neutral pions generating dynamically a $\pi\pi$ loop. This effect is doubling the cross section in the threshold region and is regarded by the authors as being a reminiscence of the explicit chiral loop effect described before.

In the past, two measurements of the reaction $\gamma p \rightarrow \pi^0\pi^0 p$ below 450 MeV beam energy have been carried out [10, 11]. The second experiment showed an improvement in statistics by almost a factor 30. Nevertheless, in the threshold region the cross section still suffered from large statistical uncertainties (see Fig. 1).

Reaction Mechanisms in the second Resonance Region

Nucleon resonances are studied in a variety of experiments in an attempt to obtain information on the structure of the nucleon by comparison to quark model calculations. Most information has been gathered through πN scattering and π photoproduction. A complementary access is the double π production where the $2\pi^0$ channel turns out to be the most selective one. Because of the vanishing charge of the π^0 , Born terms as well as direct production terms (Δ -Kroll-Rudermann, Δ -pion pole) are very much suppressed. Previously, two measurements of the reaction $\gamma p \rightarrow \pi^0\pi^0 p$ were intensively studied in order to extract information on nucleon resonances. The MAMI results [11] were interpreted by the Valencia model [8] and gave a strong indication for a dominance for the $D_{13}(1520) \rightarrow \Delta\pi$. In a recent paper, the GRAAL collaboration reported on a measurement of the $2\pi^0$ channel from 650 MeV up to 1500 MeV [12]. These data were interpreted by an extention of the Laget-Murphy model [12]. Despite the bad coverage of the $P_{11}(1440)$ resonance with the incident beam energy, the authors emphasized that the

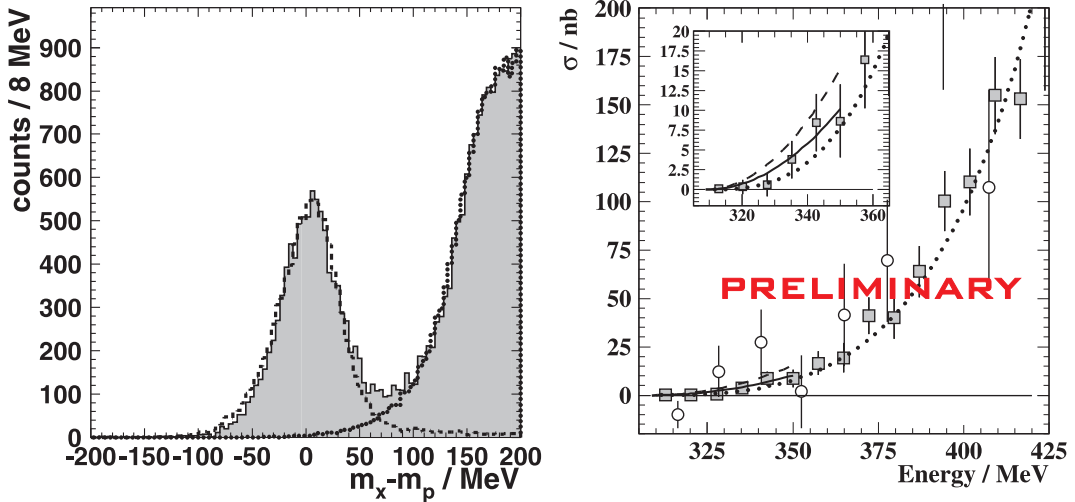


FIGURE 1. Left: Missing mass $M_X - m_p$ for two detected π^0 mesons for beam energies 780–820 MeV MeV (gray data, dashed $2\pi^0$ sim., dotted η sim.). Right: Total cross section for the reaction $\gamma p \rightarrow \pi^0\pi^0 p$ (full squares) at threshold in comparison with [11] (open circles). The prediction of the ChPT calculation [7] is shown (solid curve) together with its upper limit (dashed curve) and the prediction of Ref. [9] (dotted curve).

data could be only explained by a dominance of the $P_{11}(1440) \rightarrow \sigma N$ reaction process. We present and discuss in this paper new and very precise invariant mass distributions of the $\pi^0\pi^0$ and $\pi^0 p$ systems.

EXPERIMENTAL SETUP AND DATA ANALYSIS

The reaction $\gamma p \rightarrow \pi^0\pi^0 p$ was measured at the electron accelerator Mainz Microtron (MAMI) [13, 14] using the Glasgow tagged photon facility [15, 16] and the photon spectrometer TAPS [17, 18]. The photon energy covered the range 285–820 MeV with an average energy resolution of 2 MeV. The TAPS detector consisted of six blocks each with 62 hexagonally shaped BaF_2 crystals arranged in an 8×8 matrix and a forward wall with 138 BaF_2 crystals arranged in a 11×14 rectangle. The six blocks were located in a horizontal plane around the target at angles of $\pm 54^\circ$, $\pm 103^\circ$ and $\pm 153^\circ$ with respect to the beam axis. Their distance to the target was 55 cm and the distance of the forward wall was 60 cm. This setup covered $\approx 40\%$ of the full solid angle. The liquid hydrogen target was 10 cm long with a diameter of 3 cm. Further details of the experimental setup can be found in ref. [19].

The $\gamma p \rightarrow \pi^0\pi^0 p$ reaction channel was identified by measuring the 4-momenta of the two π^0 mesons, whereas the proton was not detected. The π^0 mesons were detected via their two photon decay channel and identified in a standard invariant mass analysis from the measured photon momenta. Events were selected, were both of the two photon invariant masses fulfilled simultaneously the following cut: $110\text{MeV} < m_{\gamma\gamma} < 150\text{MeV}$. Furthermore, the mass M_X of a missing particle was calculated (see Fig. 1). In case

of the reaction $\gamma p \rightarrow \pi^0 \pi^0 p$ the missing mass M_X must be equal to the mass of the (undetected) proton m_p . Above the η production threshold of 707 MeV, the $\eta \rightarrow 3\pi^0$ decay is a potential background source for the $2\pi^0$ channel via events where only two of the three π^0 mesons are detected by TAPS. A Monte Carlo simulation of the $2\pi^0$ and η reactions using GEANT3 [20] reproduces the line shape of the measured data. A cut corresponding to an interval of $-2.5\sigma \dots \min\{+2.5\sigma, 40\text{MeV}\}$ width of the simulated line shape has been applied to select the events of interest. The $\eta \rightarrow 3\pi^0$ background was estimated from these simulations to be below 2% for the highest beam energy of 820 MeV (compare Fig. 1) and was subtracted for the cross section determination. Background originating from random time coincidences between the TAPS detector and the tagging spectrometer was subtracted in the usual way, using events outside the prompt time coincidence window [16].

The cross section was deduced from the rate of the $2\pi^0$ events, the number of hydrogen atoms per cm^2 , the photon beam flux, the branching ratio of the π^0 decay into two photons, and the detector and analysis efficiency. The geometrical detector acceptance and the analysis efficiency due to cuts and thresholds were obtained using the GEANT3 code and an event generator producing distributions of the final state particles according to phase space. The acceptance of the detector setup was studied by examining independently a grid of the four degrees of freedom for this three body reaction (azimuthal symmetry of the reaction was assumed). In a grid of total 1024 bins the acceptance is 100% for the beam below 410 MeV and above greater than 95% for the energy up to 820 MeV. The average value for the detection efficiency is 0.4%. The systematic errors of the efficiency determination are small, because the shape of the measured distributions are reproduced by the simulation. The systematic errors are estimated to be 8% and include uncertainties of the beam flux, the target length and the efficiency determination.

RESULTS AND DISCUSSION

Chiral Perturbation Theory

The measured total cross section at threshold for the reaction $\gamma p \rightarrow \pi^0 \pi^0 p$ is shown in Fig. 1 as a function of the incident photon beam energy. The results are in agreement within the rather large error bars with a previous experiment [11]. The present data are compared with the prediction of the ChPT calculation [7] and is in agreement with it [21], although up to 20 MeV above threshold the data are somewhat lower than the ChPT prediction. The ChPT prediction using the upper limit of the coupling of the $P_{11}(1440)$ to $(\pi\pi)_{s\text{-wave}}$ can be excluded. In the future, this might be exploited to establish a better constraint on this coupling by using our result as an input. The total cross section is also compared to the calculation with the chiral unitary model [9] and shows a good agreement with this latter calculation.

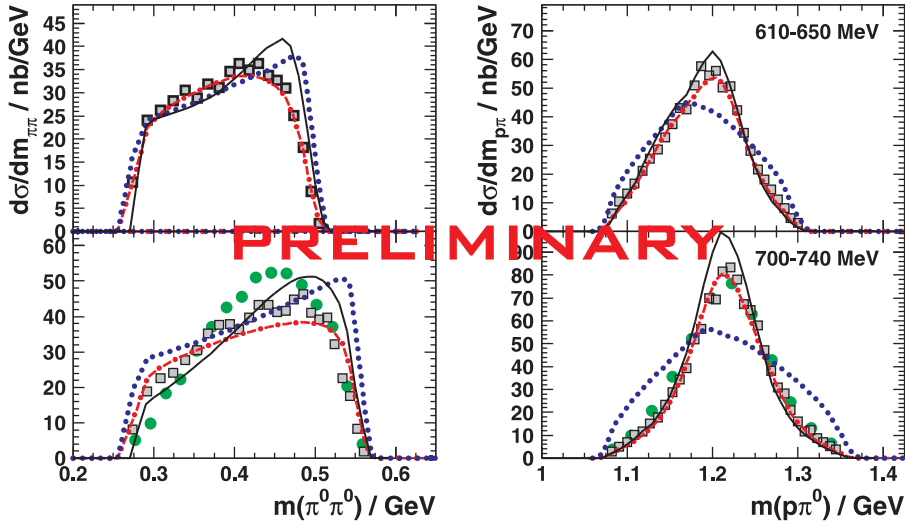


FIGURE 2. Invariant mass of $\pi^0\pi^0$ and π^0p for different bins of beam energy (full squares). The GRAAL data is shown by the full circles. The curves show σN phase space (dotted), $\Delta\pi$ phase space (dashed dotted) and the model calculation [8] (full curve).

Reaction Mechanisms in the second Resonance Region

The invariant mass distributions for two beam energies are shown in Fig. 2. They are compared to a $\Delta\pi$ phase space and a σN phase space simulations and to the Valencia model calculation [8]. For the σ a Breit-Wigner with a pole and a width of 800 MeV according to the Laget-Murphy model was assumed [22]. The GRAAL data around 720 MeV beam energy agrees very well with our m_{π^0p} data, whereas in the case of $m_{\pi^0\pi^0}$, the agreement is worse. In the m_{π^0p} distributions, the $\Delta\pi$ intermediate state dominates starting already at 600 MeV beam energy. The other phase space distributions can not describe the data. In the $m_{\pi^0\pi^0}$ distributions the differences between the different reaction processes is much less discriminative. The dominance of the $\Delta\pi$ intermediate state in the $2\pi^0$ production channel seems to be the more obvious explanation, although no interference effects are taken into account in this simplified comparisons. This observation is in contradiction to the claimed σN dominance in the Laget Model [12]. A future partial wave analysis has to clarify this discrepancy, and the presented data will provide strong constraints for solutions in the second resonance region.

Summary

In summary we have measured the total and differential cross sections for the reaction $\gamma p \rightarrow \pi^0\pi^0p$. The prediction of the ChPT calculation [7] is in agreement with our measured data [21]. The upper limit quoted for this prediction can be excluded. This finding might be exploited for a better constraint on the $P_{11}(1440)$ to s-wave $\pi\pi$ coupling. Further on, the cross section is also well reproduced by another calculation [9], where pion loops are dynamically generated.

Secondly, invariant mass distributions for $\pi^0\pi^0$ and $p\pi^0$ are presented. In the second energy region, σN phase space and hence a dominant contribution of the process $P_{11}(1440) \rightarrow \sigma p$ seems to be unlikely. The differential cross sections are very well described with a $\Delta\pi$ intermediate state. This is supported by the Valencia model, where the dominant contribution stems from the $D_{13}(1520) \rightarrow \Delta\pi$ process and is in contradiction to the Laget model [12]. In a future partial wave analysis this data could provide strong limitations on the resonance parameters up to the second resonance region.

ACKNOWLEDGMENTS

We thank the accelerator group of MAMI as well as many other scientists and technicians of the Institut fuer Kernphysik at the University of Mainz for the outstanding support. This work was supported by Schweizerischer Nationalfond, DFG Schwerpunktprogramm: "Untersuchung der hadronischen Struktur von Nukleonen und Kernen mit elektromagnetischen Sonden", SFB221, SFB443 and the UK Engineering and Physical Sciences Research Council.

REFERENCES

1. Weinberg, S., *Physica (Amsterdam)*, **96A**, 327 (1979).
2. Gasser, J., and Leutwyler, H., *Annals Phys.*, **158**, 142 (1984).
3. Jenkins, E., and Manohar, A., *Phys. Lett. B*, **255**, 558 (1991).
4. Bernard, V., et al., *Nucl. Phys. B*, **383**, 442 (1992).
5. Fettes, N., and Meissner, U.-G., *Nucl. Phys. A*, **676**, 311 (2000).
6. Bernard, V., et al., *Nucl. Phys. A*, **580**, 475–499 (1994).
7. Bernard, V., Kaiser, N., and Meissner, U., *Phys. Lett. B*, **382**, 19–23 (1996).
8. Tejedor, J. G., and Oset, E., *Nucl. Phys. A*, **600**, 413 (1996).
9. Roca, L., Oset, E., and Vacas, M. V., *Phys. Lett. B*, **541**, 77–86 (2002).
10. Haerter, F., et al., *Phys. Lett. B*, **401**, 229 (1997).
11. Wolf, M., et al., *Eur. Phys. J. A* **9** (2000) 5–8 (2000).
12. Assafiri, Y., et al., *Phys. Rev. Lett.*, **90**, 222001 (2003).
13. Walcher, T., *Prog. Part. Nucl. Phys.*, **24**, 189–203 (1990).
14. Ahrens, J., et al., *Nucl. Phys. News*, **4**, 5–15 (1994).
15. Anthony, I., et al., *Nucl. Instr. Meth.*, **A 301**, 230–240 (1991).
16. Hall, S., et al., *Nucl. Instr. Meth.*, **A 368**, 698 (1996).
17. Novotny, R., *IEEE Trans. Nucl. Sci.*, **38**, 379–385 (1991).
18. Gabler, A., et al., *Nucl. Instr. Meth.*, **A 346**, 168–176 (1994).
19. Kotulla, M., *Prog. Part. Nucl. Phys.*, **50/2**, 295–303 (2003).
20. Brun, R., et al., *GEANT3 Users Guide*, CERN, Data Handling Division DD/EE/84-1 (1986).
21. Kotulla, M., et al., *Phys. Lett. B*, **accepted** (2003).
22. Murphy, L., and Laget, J.-M., *DAPHIA-SPhN-96-10* (1996).